

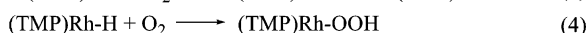
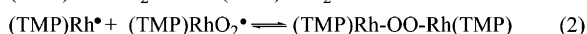
Superoxo, Peroxo, and Hydroperoxo Complexes Formed from Reactions of Rhodium Porphyrins with Dioxygen: Thermodynamics and Kinetics

Weihong Cui and Bradford B. Wayland*

Department of Chemistry, University of Pennsylvania, Philadelphia, Pennsylvania 19104-6323

Received April 25, 2006; E-mail: wayland@sas.upenn.edu

Dioxygen reactions with rhodium tetramesitylporphyrin ((TMP)Rh^{II}• (1)) and the hydride complex ((TMP)Rh–H (2)) result in formation of superoxo ((TMP)RhO₂• (3)) (eq 1), μ -peroxo ((TMP)Rh–OO–Rh(TMP) (4)) (eqs 2 and 3), and hydroperoxy ((TMP)Rh–OOH (5)) (eq 4) complexes in benzene at 300 K. The (TMP)Rh system provides an unusual opportunity to evaluate the equilibrium relationship between the superoxo and μ -peroxo complexes (eqs 1–3) and to observe the formation and reactions of the rhodium hydroperoxy species. The central role of these types of dioxygen reactions in hydrocarbon oxidations¹ and the transport and activation of oxygen in biological processes² motivates communicating these interim results.



Benzene solutions of (TMP)Rh^{II}• (1) in contact with dioxygen show ¹H NMR spectra that are interpreted in terms of mole fraction averaged positions resulting from limiting fast interchange of O₂ between 1 and a dioxygen complex, (TMP)RhO₂• (3) (eq 1) (Figure 1). Toluene solutions of 1 when exposed to dioxygen (*P*_{O₂} = 90 Torr) give EPR spectra in solution ($\langle g \rangle = 2.031$; *T* = 253 K) and glass (*g*₁ = 2.099; *g*₂ = 2.013; *g*₃ = 1.988; *T* = 90 K) that are nearly indistinguishable from the values for L(CH₃CN)RhOO²⁺ (L = *meso*-Me₆-[14]aneN₄), which has been structurally characterized as a coordinated superoxo species.³

Solutions of (TMP)Rh^{II}• (1) and O₂ in equilibrium with (TMP)RhO₂• (3) are meta-stable with respect to the very slow formation of a diamagnetic complex assigned as the μ -peroxo complex ((TMP)Rh–OO–Rh(TMP) (4))⁴ (eqs 2 and 3). Rapid formation of the μ -peroxo complex of rhodium octaethylporphyrin ((OEP)Rh–OO–Rh(OEP))⁵ from reaction of [(OEP)Rh]₂ and O₂ suggests that the steric demand of the tetramesitylporphyrin ligand leads to a kinetic barrier to produce the μ -peroxo derivative from reaction of 1 and 3.

Changes in the ¹H NMR shifts for the pyrrole and *p*-methyl hydrogens (δ_{pyrrole} and $\delta_{p\text{-CH}_3}$) as a function of the molar concentration of O₂ are accurately fitted to an expression derived for the 1:1 equilibrium (eq 1) (Figure 2). Excellent agreement between the equilibrium constants (*K*₁(300 K))⁶ evaluated from two independent observables (*K*₁(pyrr) = 8.4(0.5) × 10³, *K*₁(*p*-CH₃) = 8.5(0.4) × 10³; *T* = 300 K)⁶ provides confidence that the equilibrium between 1 and 3 is accurately described. Equilibrium constants for producing the μ -peroxo complex 4 from reaction of 1 and 3 (eq 2) (*K*₂ = 1.2(0.6) × 10³)⁶ and from the overall reaction (eq 3) (*K*₃ = 1.0(0.6) × 10⁷)⁶ are evaluated by integration of the ¹H NMR at equilibrium at 300 K.

Reaction of the hydride complex (TMP)Rh–H (2) in benzene with O₂ produces a transient diamagnetic species identified as the

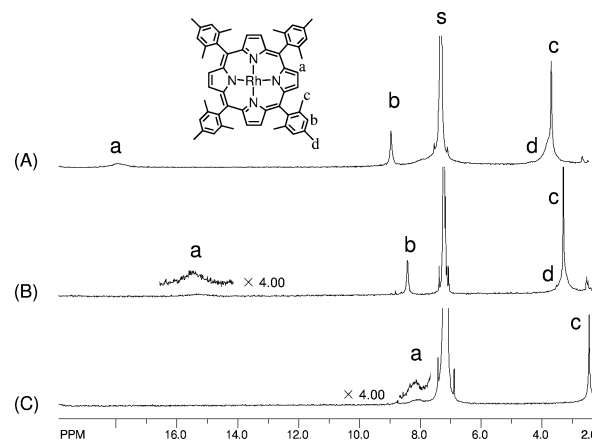


Figure 1. Proton NMR spectra for a benzene solution of (TMP)Rh• (1.0 × 10^{−3} M) at 300 K: (A) absence of O₂; (B) 6 Torr of O₂; (C) 760 Torr of O₂.

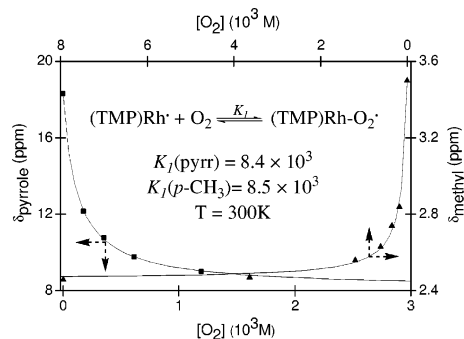
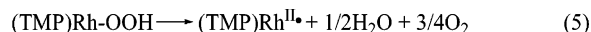


Figure 2. Fast exchange mole fraction averaged ¹H NMR chemical shifts for the pyrrole (■) and *p*-methyl (▲) hydrogens of (TMP)Rh• (1) and (TMP)Rh–O₂• (3) in C₆D₆ as a function of [O₂] at 300 K ([TMP] = 1.0 × 10^{−3} M). The solid curves are the calculated nonlinear least-squares best fit lines for *K*₁, δ_1 , and δ_3 fitted to the equation for 1:1 equilibrium: $\delta_{\text{obs}} = (\delta_1 + K_1[\text{O}_2]\delta_3)/(1 + K_1[\text{O}_2])$, in which δ_1 and δ_3 are the ¹H NMR shifts of for species 1 and 3, respectively.

hydroperoxy complex (TMP)Rh–OOH (5).⁷ The ¹H NMR resonance at −0.30 ppm that is absent in the deuterated derivative ((TMP)Rh–OOD) is assigned to the hydroperoxy hydrogen. A kinetic study for the reaction of 2 with O₂ is shown in Figure 3. Disappearance of the hydride 2 is accompanied by formation of the transient hydroperoxy complex 5, which decays to an equilibrium distribution of 1 and 3. The kinetic observations in Figure 3 are accurately fitted to a pathway where the hydroperoxy complex 5 is formed by direct reaction of O₂ with 2 followed by an apparent first-order decay of the hydroperoxy complex 5 to products (TMP)Rh^{II}•, H₂O, and O₂ (eqs 4 and 5).



The rate law for reaction 4 ($-d[\text{Rh–H}]/dt = k_4[\text{Rh–H}][\text{O}_2]$) is consistent with a direct reaction of (TMP)Rh–H with O₂. Hydrogen

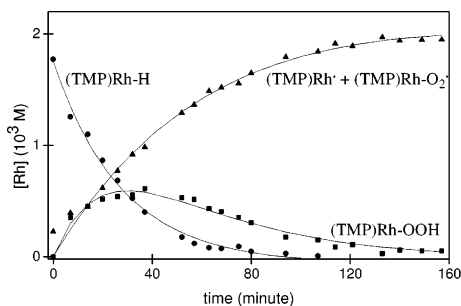


Figure 3. Change of concentrations of (TMP)Rh–H (●), (TMP)Rh–OOH (■), and the paramagnetic (TMP)Rh species (▲) with time in the reaction of (TMP)Rh–H with O₂ (680 Torr) in benzene at 300 K ([TMP] = 1.0 × 10⁻³ M). The solid curves are the nonlinear least-squares best fit lines for the solution species, which provide rate constants of k_4 and k_5 as 7.1(1.0) × 10⁻² M⁻¹s⁻¹ and 4.7(1.4) × 10⁻⁴ s⁻¹, respectively.

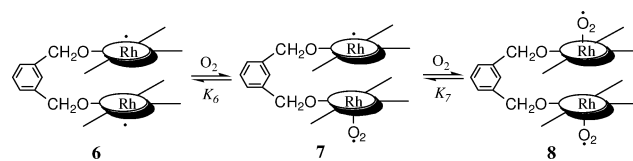
atom transfer from Rh–H to a superoxo oxygen (RhO₂•) was the anticipated route to form the hydroperoxy complex (Rh–OOH) because of several similar precedents,⁸ but the kinetic study clearly indicates that an alternate pathway is operating in the (TMP)Rh system. The sterically demanding mesityl groups must inhibit (TMP)Rh–H and (TMP)RhO₂• from reaching the transition state for hydrogen transfer. A small deuterium isotope effect ($k_{4(H)}/k_{4(D)} = 1.5$) and the rate law observed for reaction 4 are most consistent with a near concerted addition of O₂ to the Rh–H unit through a low symmetry transition state.

The hydroperoxy complex (TMP)Rh–OOH is a transient that reacts on to form water and (TMP)Rh^{II}• (1), which contrasts with most transition metal hydroperoxy complexes that produce a hydroxide complex (MOOH → MOH + 1/2O₂).⁹ Reaction of H₂ and O₂ is catalyzed by 1 as evidenced by the growth of the broad ¹H NMR resonance for H₂O at 0.38 ppm, but formation of H₂O proceeds slowly because the reaction of 1 with H₂ is a rate-limiting termolecular process.¹⁰ Tethered dirhodium(II) diporphyrin complexes with three mesityl groups per porphyrin unit have sterics similar to those of rhodium(II) tetramesitylporphyrin ((TMP)Rh^{II}•) and give fast bimolecular reactions with H₂,¹¹ which provides a better opportunity to illustrate catalytic behavior involving dihydrogen.

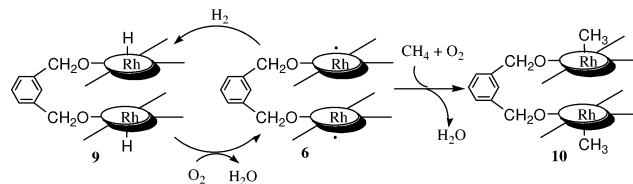
The *m*-xylyl-tethered dirhodium(II) diporphyrin complex (•Rh(*m*-xylyl)Rh• (6)) reacts reversibly with O₂ to form mono- and bis-dioxygen complexes (•Rh(*m*-xylyl)Rh–O₂• (7) and •O₂–Rh(*m*-xylyl)Rh–O₂• (8)) (Scheme 1). The equilibrium constants ($K_6 = 1.5(0.4) \times 10^4$; $K_7 = 7.4(0.2) \times 10^3$; $T = 300$ K)⁶ for the sequential dioxygen complex formation were evaluated from the nonlinear least-squares curve fitting of the observed mole fraction averaged chemical shifts to the equation: $\delta_{\text{obs}} = (\delta_6 + K_6[\text{O}_2]\delta_7 + K_6K_7[\text{O}_2]^2\delta_8)/(1 + K_6[\text{O}_2] + K_6K_7[\text{O}_2]^2)$, where δ_6 , δ_7 , and δ_8 are the ¹H NMR shifts for species 6, 7, and 8, respectively. The observed ratio of approximately 2 for K_6/K_7 is the expected statistical result when the two rhodium(II) centers are fully independent.

Reaction of •Rh(*m*-xylyl)Rh• (6) with H₂ forms the dihydride derivative H–Rh(*m*-xylyl)Rh–H (9) rapidly, and 9 reacts readily with O₂ to form water and regenerate 6 without observing a hydroperoxy intermediate. Mixtures of H₂ ($P_{\text{H}_2} > 300$ Torr) and O₂ ($P_{\text{O}_2} < 30$ Torr) react with 6 to produce water catalytically until the O₂ is essentially consumed, and the residual H₂ reacts with 6 to form the dihydride complex 9 (Scheme 2). Reaction of 6 with CH₄ and O₂ ($P_{\text{CH}_4} > 300$ Torr, $P_{\text{O}_2} < 30$ Torr) produces only a stoichiometric quantity of H₂O and the dimethyl complex CH₃–Rh(*m*-xylyl)Rh–CH₃ (10) (Scheme 2), which does not react thermally with O₂ at a finite rate at 300 K.

Scheme 1



Scheme 2



More complete thermodynamic and mechanistic studies for dioxygen and hydroperoxy complex formation and an effort to evaluate the utility of these species in substrate oxidation reactions are in progress.

Acknowledgment. This research was supported by the Department of Energy, Division of Chemical Sciences, Office of Science through Grant DE-FG02-86ER-13615.

Supporting Information Available: Equilibrium measurements for the dioxygen binding process to rhodium(II) metalloradicals, the expressions for the kinetics study of (TMP)Rh–H with dioxygen, and characterization data for compounds 1–10. This material is available free of charge via the Internet at <http://pubs.acs.org>.

References

- (1) (a) Sheldon, R. A.; Arends, I.; Ten Brink, G. J.; Dijkstra, A. *Acc. Chem. Res.* **2002**, *35*, 774–781. (b) Stahl, S. S. *Angew. Chem., Int. Ed.* **2004**, *43*, 3400–3420. (c) Simandi, L. I. *Advances in Catalytic Activation of Dioxygen by Metal Complexes*; Kluwer Academic Publishers: Dordrecht, The Netherlands, 2003; Vol. 26, p 336. (d) Velusamy, S.; Srinivasan, A.; Punniyamurthy, T. *Tetrahedron Lett.* **2006**, *47*, 923–926. (e) Punniyamurthy, T.; Velusamy, S.; Iqbal, J. *Chem. Rev.* **2005**, *105*, 2329–2363.
- (2) (a) Lippard, S. J.; Berg, J. M. *Principles of Bioinorganic Chemistry*; University Science: Mill Valley, CA, 1995. (b) Que, L., Jr.; Tolman, W. B., Eds. *Comprehensive Coordination Chemistry II: BioCoordination Chemistry*; Elsevier: London, 2004; Vol. 8.
- (3) Bakac, A.; Guzei, I. A. *Inorg. Chem.* **2000**, *39*, 736–740.
- (4) (TMP)Rh–OO–Rh(TMP) (4): ¹H NMR (C₆D₆) δ (ppm) 8.27 (s, 8H, pyrrole), 7.21 (s, 4H, *m*-phenyl), 6.93 (s, 4H, *m*-phenyl), 2.41 (s, 12H, *p*-CH₃), 1.92 (s, 12H, *o*-CH₃), 1.20 (s, 12H, *o'*-CH₃).
- (5) Wayland, B. B.; Newman, A. R. *J. Am. Chem. Soc.* **1979**, *101*, 6472–6473.
- (6) All equilibrium constants (K_1 , K_2 , K_3 , K_6 , K_7) are based on the standard state of 1 M for each constituent. Equilibrium constants are dimensionless, but are sometimes given nominal units associated with the standard state. (Nominal units are M⁻¹ for K_1 , K_2 , K_6 , and K_7 , and M⁻² for K_3).
- (7) (TMP)Rh–OOH (5): ¹H NMR (C₆D₆) δ (ppm) 8.90 (s, 8H, pyrrole), 2.45 (s, 12H, *p*-CH₃), 2.24 (s, 12H, *o*-CH₃), 1.99 (s, 12H, *o'*-CH₃), –0.30 (br, 1H, Rh–OOH), the *m*-phenyl hydrogens are obscured by solvent peak.
- (8) (a) Bakac, A. *J. Am. Chem. Soc.* **1997**, *119*, 10726–10731. (b) Endicott, J. F.; Wong, C. L.; Inoue, T.; Natarajan, P. *Inorg. Chem.* **1979**, *18*, 450–454.
- (9) (a) Denney, M. C.; Smythe, N. A.; Cetto, K. L.; Kemp, R. A.; Goldberg, K. I. *J. Am. Chem. Soc.* **2006**, *128*, 2508–2509. (b) Wick, D. D.; Goldberg, K. I. *J. Am. Chem. Soc.* **1999**, *121*, 11900–11901. (c) Thyagarajan, S.; Incarvito, C. D.; Rheingold, A. L.; Theopold, K. H. *Chem. Commun.* **2001**, 2198–2199. (d) Rostovtsev, V. V.; Henling, L. M.; Labinger, J. A.; Bercaw, J. E. *Inorg. Chem.* **2002**, *41*, 3608–3619. (e) Atlay, M. T.; Preece, M.; Strukul, G.; James, B. R. *Can. J. Chem.* **1983**, *61*, 1332–1338. (f) Pregagli, G.; Morelli, D.; Conti, F.; Gregorio, G.; Ugo, R. *Faraday Discuss.* **1968**, 110.
- (10) Wayland, B. B.; Ba, S. J.; Sherry, A. E. *Inorg. Chem.* **1992**, *31*, 148–150.
- (11) (a) Cui, W. H.; Wayland, B. B. *J. Am. Chem. Soc.* **2004**, *126*, 8266–8274. (b) Zhang, X. X.; Wayland, B. B. *J. Am. Chem. Soc.* **1994**, *116*, 7897–7898.

JA0628755